Journal of Magnetic Resonance 206 (2010) 88–96

Contents lists available at ScienceDirect

Journal of Magnetic Resonance

journal homepage: www.elsevier.com/locate/jmr

Effects of in-pulse transverse relaxation in 3D ultrashort echo time sequences: Analytical derivation, comparison to numerical simulation and experimental application at 3 T

Fabian Springer [a,b,*], Günter Steidle [a], Petros Martirosian [a], Claus D. Claussen [b], Fritz Schick [a]

[a] Section on Experimental Radiology, Department of Diagnostic and Interventional Radiology, University Hospital, 72076 Tübingen, Germany
[b] Department of Diagnostic and Interventional Radiology, University Hospital, 72076 Tübingen, Germany

ARTICLE INFO

Article history:
Received 27 August 2009
Revised 21 May 2010
Available online 23 June 2010

Keywords:
Ultrashort echo time imaging
UTE
In-pulse relaxation effects
Ernst equation for fast spoiled gradient echo sequences
Measurement of longitudinal relaxation time

ABSTRACT

The introduction of ultrashort-echo-time-(UTE)-sequences to clinical whole-body MR scanners has opened up the field of MR characterization of materials or tissues with extremely fast signal decay. If the transverse relaxation time is in the range of the RF-pulse duration, approximation of the RF-pulse by an instantaneous rotation applied at the middle of the RF-pulse and immediately followed by free relaxation will lead to a distinctly underestimated echo signal. Thus, the regular Ernst equation is not adequate to correctly describe steady state signal under those conditions. The paper presents an analytically derived modified Ernst equation, which correctly describes in-pulse relaxation of transverse magnetization under typical conditions: The equation is valid for rectangular excitation pulses, usually applied in 3D UTE sequences. Longitudinal relaxation time of the specimen must be clearly longer than RF-pulse duration, which is fulfilled for tendons and bony structures as well as many solid materials. Under these conditions, the proposed modified Ernst equation enables adequate and relatively simple calculation of the magnetization of materials or tissues. Analytically derived data are compared to numerical results obtained by using an established Runge–Kutta-algorithm based on the Bloch equations. Validity of the new approach was also tested by systematical measurements of a solid polymeric material on a 3 T whole-body MR scanner. Thus, the presented modified Ernst equation provides a suitable basis for $T1$ measurements, even in tissues with $T2$ values as short as the RF-pulse duration: independent of RF-pulse duration, the 'variable flip angle method' led to consistent results of longitudinal relaxation time $T1$, if the $T2$ relaxation time of the material of interest is known as well.

1. Introduction

Recently introduced ultrashort-echo-time-(UTE)-sequences have the potential to visualize a variety of tissues and materials (e.g. cortical bone, solid polymeric materials) on clinically used whole-body MR scanners [1–4]. Applying these UTE sequences, tissues with an extremely fast signal decay cannot only be visualized by means of magnetic resonance imaging (MRI), but also characterized regarding their transverse and longitudinal relaxation times as well as possible magnetization transfer effects [5]. In three-dimensional (3D)-UTE-imaging, a short rectangular radiofrequency (RF) pulse is often used for non-slice-selective excitation of the tissue followed by centric radial or spiral k-space sampling [6–9]. For parenchymal tissues and fluids with long transverse relaxation times ($T2$) the steady state signal can be adequately described by the well-known regular Ernst equation for spoiled gradient-echo-sequences, if "ideal" spoiling of transverse magnetization before each single excitation pulse can be assumed [10–12].

In materials or tissues with extremely short transverse relaxation time, marked relaxation of transverse magnetization takes place already during RF excitation which leads to so called in-pulse relaxation effects: the regular Ernst equation, in which the RF-pulse effect is represented by a simple instantaneous rotation of the magnetization vector and immediately followed by free relaxation, is not valid anymore, since it will lead to a distinctly underestimated echo signal at echo time TE. Thus, the regular Ernst equation is not adequate to correctly describe steady state signal under those conditions and has to be replaced by a modified version of the Ernst equation, which additionally accounts for marked effects of in-pulse relaxation. Thus, only a modified Ernst equation will allow for accurate assessment of the course of magnetization and determination of longitudinal relaxivity by means of the 'variable flip angle method' in specimen with transverse relaxation times similar to the RF-pulse duration.

* Corresponding author. Address: University Hospital Tübingen, Department of Diagnostic and Interventional Radiology, Section on Experimental Radiology, Hoppe-Seyler-Str. 3, 72076 Tübingen, Germany. Fax: +49 7071 295392.
E-mail address: Fabian.Springer@med.uni-tuebingen.de (F. Springer).

1090-7807/$ - see front matter © 2010 Elsevier Inc. All rights reserved.
doi:10.1016/j.jmr.2010.06.010

In this study, an analytically derived, modified version of the Ernst equation for fast spoiled GRE-sequences is presented taking into account effects of transverse in-pulse relaxation. Numerical simulations were performed by using an established Runge–Kutta-algorithm based on the Bloch equations and results were compared to those analytically obtained using the regular and the modified Ernst equation.

By means of a 3D UTE sequence, signal intensities from a sample of solid polymeric material were recorded on a 3 T whole-body MRI unit applying a variety of nominal flip angles at different durations of the RF excitation pulse. Longitudinal relaxation time ($T1$) was calculated by fitting the regular and modified Ernst equation to the series of signal intensities recorded with variable nominal flip angles.

2. Materials and methods

2.1. Regular and modified Ernst equation

The signal yield using fast spoiled gradient echo sequences can be described by the regular Ernst equation, if the following prerequisites are fulfilled: $T1$ and $T2^*$ of the investigated tissue have to be much longer than the duration of the applied RF excitation pulse (T_{RF}), repetition time (TR) is clearly longer than $T2^*$ (transverse magnetization has vanished when the next RF-pulse is applied or "ideal" spoiling can be assumed) and signal is acquired when steady state conditions are reached [10–12]:

$$M_{TR} = M_\infty \cdot \frac{(1 - E1) \cdot \sin\alpha}{1 - E1 \cdot \cos\alpha} \cdot e^{\frac{-TE}{T2^*}} \quad (1)$$

with $E1 = e^{-TR/T1}$ and nominal flip angle α.

This equation essentially consists of terms describing the amount of magnetization which is "converted" from the longitudinal into the transverse direction, if steady state conditions are reached. These terms are followed by the effective mono-exponential signal decay between RF-pulse and signal acquisition under free relaxation conditions.

However, relaxation processes during the RF excitation pulse must be additionally considered, if spin–spin ($T2$) or spin–lattice ($T1$) relaxation time of the material under investigation is not much longer than the RF-pulse duration. Since in many cases longitudinal relaxation time $T1$ is much longer than the duration of the RF excitation pulse T_{RF} [2,13], the effect of longitudinal relaxation during the RF excitation pulse will be neglected in this work and this assumption is further discussed later on. For significant transverse relaxation effects during rectangular RF excitation the sine and cosine terms have to be modified as shown in Appendix 1:

$$\sin(\alpha) \rightarrow b = e^{-\tau} \cdot \frac{\alpha}{\Phi} \cdot \sin(\Phi)$$

$$\cos(\alpha) \rightarrow a = e^{-\tau} \cdot \left[\cos(\Phi) + \frac{\tau}{\Phi} \cdot \sin(\Phi)\right]$$

Φ is derived from the nominal flip angle α (in radians) by the following equations: $\Phi = \sqrt{\alpha^2 - \tau^2}$ and $\tau = T_{RF}/(2 \cdot T2^*)$. Thus, the regular Ernst equation is transferred into the modified Ernst equation, which also considers significant transverse relaxation effects during a rectangular RF excitation pulse:

$$M_{TR} = M_\infty \frac{(1 - E1) \cdot b}{1 - E1 \cdot a} \cdot e^{\left(-\left(\frac{TE}{T2^*} - \tau\right)\right)} \quad (2)$$

The term $M_\infty \frac{(1-E1)}{1-E1 \cdot a}$ refers to the longitudinal steady state magnetization before the excitation pulse, the term $M_\infty \frac{(1-E1)}{1-E1 \cdot a} \cdot b$ refers to the converted transverse and $M_\infty \frac{(1-E1)}{1-E1 \cdot a} \cdot a$ to the residual longitudinal magnetization after the excitation pulse.

To be in accordance with the regular Ernst equation, the echo time (TE) is defined as the time from centre of the RF excitation pulse to the point when central k-space data is acquired.

Obviously, the modified Ernst equation (Eq. (2)) equals the regular Ernst equation (Eq. (1)), if the transverse relaxation time $T2^*$ is much longer than the duration of the rectangular RF excitation pulse T_{RF}. In this case τ approaches zero and thus no in-pulse relaxation effects of transverse magnetization can be observed.

In the presented study, effects of the modified Ernst equation on resulting longitudinal and transverse magnetization in the steady state were studied and compared to results from the regular Ernst equation. Since only the ratio of RF-pulse duration to transverse relaxation time ($T_{RF}/T2^*$) and the ratio of repetition time to longitudinal relaxation time ($TR/T1$) are relevant in Eq. (2), variations of those ratios were evaluated in the following.

2.2. Numerical simulation

The analytically derived modified Ernst equation (Eq. (2)) was compared to results from a numerical simulation using an established Runge–Kutta-algorithm, which was implemented in a home-written C++ program. The numerical simulation was based on a five-stage Runge–Kutta algorithm with fourth-order accuracy, step width was set to one microsecond. The transverse magnetization at the beginning of the RF-pulse was set to zero in our simulation, since in materials and tissues with extremely small $T2^*$ values the created transverse magnetization has completely vanished before the beginning of the next RF excitation pulse. Transverse magnetization was assessed when steady state conditions were reached (after at least 100 excitation cycles).

Numerical calculations were based on a timing with $TR = T_{RF} + d_1 + d_2$ (Fig. 1). In this timing scheme T_{RF} represents the total duration of the rectangular RF excitation, d_1 represents the period of free relaxation between the end of the rectangular RF excitation pulse and the time point when central k-space data is acquired (beginning of readout period, before starting the spatial encoding gradient in centric radial UTE sequences). The time interval d_2 represents the remaining time until the starting point of the next RF excitation pulse. For real sequences a delay time ($d_1 = 0.02$ ms) between the end of the rectangular excitation pulse and starting of signal readout has to be considered as a scanner specific time constant, which is needed for switching from transmit to receive mode.

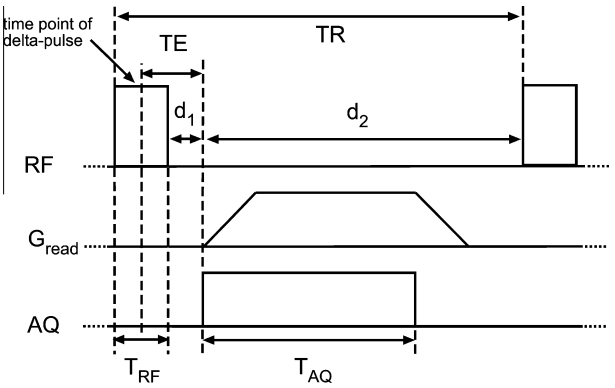

Fig. 1. 3D UTE sampling scheme: A rectangular radiofrequency (RF) excitation block pulse with duration T_{RF} is followed by 3D centric radial sampling of the k-space data (T_{AQ}) after echo time $TE = T_{RF}/2 + d_1$; schematically drawn are read gradients (G_{read}) and acquisition window (AQ). Delay time d_1 between end of RF excitation pulse and acquisition of centric k-space data; d_2 between begin of centric k-space acquisition and next RF excitation. For comparison, the case of an infinitesimally short "delta" RF-pulse in the middle of time period T_{RF}, as considered by analytical calculations with the regular Ernst equation, is also depicted.

In numerical simulations, transverse relaxation times were varied between $T2^* = 0.02$ ms and $T2^* = 100$ ms in order to assess effects of transverse in-pulse relaxation. Transverse magnetization was evaluated in a range of nominal flip angles between 5° and 90° at a set of constant parameters ($T_{RF} = 0.2$ ms, TE = 0.12 ms, TR = 6.1 ms, $T1 = 150$ ms). In this context, it should be mentioned that for long $T2^*$ values ($T2^* = 100$ ms) and relatively short repetition times (TR = 6.1 ms) the assumption that transverse magnetization has completely vanished before the next RF-pulse is no longer valid. However, signal spoiling as usually implemented in UTE sequences provides (nearly) negligible transverse interferences, even in cases with $T2^* \approx$ TR.

Furthermore, in a second simulation the repetition time TR was varied between TR = 6 ms and TR = 50 ms at a constant set of parameters ($T2^* = 0.26$ ms, TE = 0.42 ms, $T_{RF} = 0.8$ ms, $T1 = 150$ ms).

In the analytical derivation of the modified Ernst equation, longitudinal relaxation during RF excitation was assumed to be negligible (Appendix 1). Therefore, it had to be tested which minimum $T1/T_{RF}$ ratio is tolerable regarding the practical use of the proposed modified Ernst equation. For nominal flip angles between 5° and 90° (flip angle increment of 5°) and different ratios of $T1/T_{RF} = (10, 5, 1)$, we investigated differences between numerical simulations and results obtained using the modified Ernst equation. For this evaluation repetition time was set to TR = (100, 10, 1) ms, echo time and RF-pulse duration were set to TE = 0.07 ms and $T_{RF} = 0.1$ ms, respectively. For all investigated $T1/T_{RF}$ ratios and the three investigated repetition times, an additional influence of $T2^*/T_{RF}$ on the longitudinal in-pulse relaxation was also evaluated by setting $T2^* = T1$ (for the longest possible transverse relaxation time) or $T2^* = 0.1$ ms (with $T_{RF} = 0.1$ ms) for marked in-pulse relaxation of transverse magnetization. Calculated differences between numerical simulation and modified Ernst equation were considered relevant, if signal intensities from the modified Ernst equation differed by more than ~2% from the numerically calculated transverse magnetization.

3. Experimental setting

3.1. MRI scanner and specimen

All images were recorded on a 3 T whole-body scanner (MAGNETOM Trio, Siemens Healthcare, Erlangen, Germany). The maximum gradient strength was 45 mT/m along each orthogonal axis with a maximum gradient slew rate of 200 T/m/s. A sample of solid polymeric material (Polyurethane: PUR) was examined and positioned close to the centre of an eight channel circularly polarized transmit/receive extremity coil (Intermagnetics General Corporation, New York, USA). The coil itself was placed in the isocenter of the horizontal bore (free diameter of 60 cm) of the magnet and of the gradient system. PUR was used since it shows a fast and almost mono-exponential signal decay ($T2^* < 0.5$ ms), combined with a relatively long longitudinal relaxation time ($T1 > 100$ ms) [2]. For transmitter and receiver adjustment a 3%-agar containing tube was positioned inside the scanner, since the solid polymeric material did not provide sufficient signal intensity to allow for automatic transmitter adjustments by the clinical MR system. After transmitter adjustment the agar tube was subsequently removed and replaced by the cylindrical solid polymeric specimen, positioned with its axis along the static magnetic field in order to avoid potential susceptibility effects.

3.2. Sequence design

All images were recorded by means of a 3D UTE spoiled gradient echo sequence with centric radial k-space sampling. After rectangular RF excitation (minimal pulse duration $T_{RF} = 0.1$ ms) and the delay needed for switching from transmit to receive mode ($d_1 = 0.02$ ms), the sequence begins to acquire data points in k-space as soon as the readout gradient starts to ramp up (Fig. 1). Every radial projection starts in the centre of k-space and acquires 128 complex data points in each half projection with an oversampling factor of two. All images were acquired with the following parameters: FoV = 128 mm, isotropic resolution 1 mm, readout bandwidth was 2370 Hz/pixel resulting in a duration of the readout window of $T_{AC} = 0.422$ ms per each half projection.

In all measurement series the nominal flip angle was varied between 5° and the maximum achievable nominal flip angle, which was limited by either restrictions of SAR (specific absorption rate) or the maximum allowed transmitter voltage of the coil. Three measurement series with variable flip angle excitation (flip angle increment of 5°) were performed using RF-pulse durations of $T_{RF} = 0.1$ ms, 0.2 ms or 0.4 ms.

3.3. Analysis of acquired data

For each investigated RF-pulse duration the modified Ernst equation (Eq. (2)) as well as the regular Ernst equation (Eq. (1)) were fitted to the obtained signal yield at various flip angles. The routine uses a home-written MATLAB algorithm (*The MathWorks Inc., Matick, MA*) applying a least-square approach for fitting. Fitted parameters were M_∞ and longitudinal relaxation time $T1$. Values for RF-pulse duration T_{RF} and repetition time TR were known from pulse sequence. Furthermore, $T2^*$ had to be determined separately using the routine described in the next section.

3.4. Transverse relaxation time measurement

Correct prediction of in-pulse relaxation effects (i.e. calculation of terms a and b in Eq. (2)) requires knowledge about $T2^*$ of the specimen. Measurement of $T2^*$ was done by means of a 3D UTE sequence with $T_{RF} = 0.1$ ms, TR = 10 ms, nominal flip angle was set to the angle with the experimentally determined greatest signal yield ($\alpha = 20°$ for PUR at $T_{RF} = 0.1$ ms). Transverse relaxation time ($T2^*$) was calculated from a set of signal intensities recorded by using fifteen different delay times in a range between $d_1 = 0.02$ ms and $d_1 = 1.42$ ms (with an increment of 0.1 ms). Assuming a mono-exponential decay the signal intensity S_{d1} is described as:

$$S_{d_1} = S_0 \cdot \exp\left(-\frac{d_1}{T2^*}\right) \tag{3}$$

Noise correction was performed as described below and $T2^*$ values were calculated on a pixel-by-pixel basis according to Eq. (3) applying a least-square approach for fitting. For this task home-made *MATLAB* (*The MathWorks Inc., Matick, MA*) image processing routines were applied.

3.5. Noise correction of magnitude images

Noise contributions to signal intensities, measured in magnitude images with a low signal-to-noise ratio, might lead to systematic errors in relaxometry. For this reason all acquired images were noise corrected before further post-processing [14] on a pixel-by-pixel basis according to Eq. (4):

$$S_{\text{Corr.}} = \sqrt{(S_{\text{Uncorr.}})^2 - (S_{\text{Noise}})^2} \tag{4}$$

S_{Noise} describes the arithmetic mean of the background signal measured in four ROIs (each about 100 pixel) placed around the investigated sample in an object free, homogenous area without any artifacts. $S_{\text{Uncorr.}}$ is the uncorrected (measured) signal intensity of each pixel and $S_{\text{Corr.}}$ represents the respective noise corrected signal intensity of each pixel.

4. Results

4.1. Analytical simulation

In Fig. 2A the expressions a and b can be regarded as a measure for longitudinal (M_{tr}) and transverse (M_z) magnetization, respectively, directly after application of a single RF-pulse. In contrast, Fig. 2B shows the trajectory of longitudinal and transverse magnetization in case of steady state conditions, as described above. In both figures longitudinal and transverse magnetization are evaluated without considering additional effects of echo time TE. As intuitively expected, it can be seen that for increasing values of τ and for the same nominal flip angle α, $T2^*$ relaxation during the RF-pulse reduces the transverse magnetization (described by the term b), but also less magnetization is rotated and a larger residual longitudinal magnetization remains (described by the term a). The transverse steady state signal is decreased for decreasing values of $T2^*$. However, if echo time TE is additionally considered and defined from the centre of a rectangular RF-pulse to the time point when central k-space data is acquired (as usually done no matter if RF-pulse duration is finite or infinitesimal short) behavior of transverse magnetization becomes different as shown in Fig. 2C and D. If the effective transverse relaxation time $T2^*$ is in the range of the pulse duration, the approximation of the RF-pulse by a simple rotation matrix applied at the time of the centre of the pulse will become incorrect. The resulting transverse magnetization is distinctly underestimated at time point TE. This results from the fact that for nominal flip angle between 0° and 90° transverse signal loss during excitation is always less pronounced than for the free relaxation case. Exemplarily the temporal development of transverse steady state magnetization is shown in Fig. 2D.

Results from analytical simulations regarding different ratios of both $T_{RF}/T2^*$ and TR/$T1$ as well as variable nominal flip angles are exhibited in Fig. 3. The absolute difference between the maximum achievable signal intensity using a rectangular RF-pulse (with duration T_{RF}) and an infinitesimal short RF-pulse (applied in the middle of the time period T_{RF}) reaches for the ratio $T_{RF}/T2^*$ a local maximum at $T_{RF}/T2^* \approx 2.34$ for various conditions of TR/$T1$ (Figs. 3B and 4A). In contrast, the higher the ratio TR/$T1$ the larger is also the absolute difference in maximum achievable normalized signal between both approaches (Fig. 3E), but there is no ratio at which a local maximum is reached. In contrast to conditions where no in-pulse relaxation of transverse magnetization occurs, it can be seen that for longer RF-pulse durations (and a constant $T2^*$) the nominal flip angle should be adjusted to clearly higher values than predicted by the regular Ernst equation in order to obtain maximum achievable transverse magnetization (Fig. 3C). Applying longer TR (at a constant $T1$) shifts the nominal flip angle with maximum normalized signal also to higher nominal flip angles for both the regular and modified Ernst equation (Fig. 3D). However, small difference in the Ernst angles between both equations can still be observed (Fig. 3F).

In summary, especially in cases of pronounced in-pulse relaxation, the regular and modified Ernst equation differ markedly in the predicted signal yield as well as in the nominal flip angle at which the signal intensity is maximized (Figs. 3 and 4).

4.2. Numerical simulation

Numerical simulations based on the Bloch equations were performed in order to compare the numerical results with the predictions by the modified Ernst equation. Under the condition that

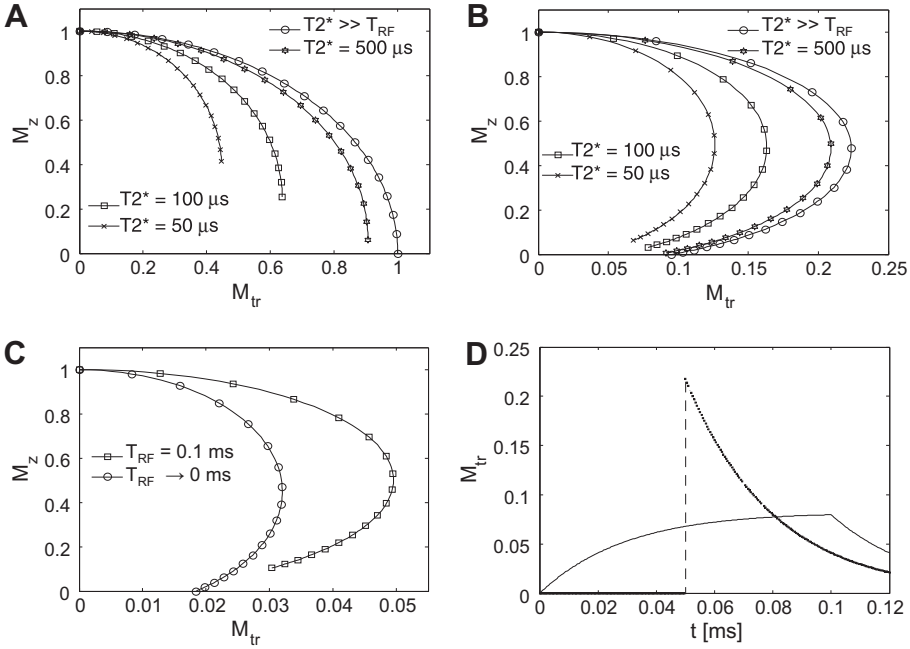

Fig. 2. (A) Shows the trajectories of the (normalized) magnetization after application of a rectangular RF-pulse of duration T_{RF} = 100 µs. Markers indicate the situation for nominal flip angles alpha = 0°, 5°, 10°, ... 85° and 90°. Trajectories are shown for various values of $T2^*$ = 50, 100, 500 µs and $T2^*$ much larger than T_{RF}. In this plot the expressions a and b can be seen as a measure for longitudinal (M_z) and transverse (M_{tr}) magnetization, respectively, after the RF-pulse (see comment #2). (B) Shows the trajectory of the steady state magnetization after application of a rectangular RF-pulse of duration T_{RF} = 100 µs. Markers indicate nominal flip angles alpha = 0°, 5°, 10°, ... 85° and 90°. Trajectories are shown for various values of $T2^*$ = 50, 100, 500 µs and $T2^*$ much larger than T_{RF}. In this plot the expressions $\frac{(1-E1)}{1-E1\cdot a}\cdot a$ and $\frac{(1-E1)}{1-E1\cdot a}\cdot b$ with the ratio TR/$T1$ = 0.1 are shown, corresponding to the longitudinal and transverse magnetization, respectively, directly after the RF-pulse in the steady state. (C) Shows, in contrast to the A and B, the behavior of transverse and longitudinal steady state magnetization after a rectangular RF-pulse (finite duration T_{RF} = 0.1 ms (squares) or infinitesimal short $T_{RF} \sim 0$ (circles)) at various flip angles followed by a short period of free relaxation; parameters were $T2^*$ = 0.03 ms, TE = 0.07 ms and TR/$T1$ = 0.1. To further illustrate this effect, in D the temporal development of the transverse steady state magnetization during a rectangular RF-pulse is exemplarily shown for a nominal flip angle α = 20° (solid line); all other parameters were the same as in C. The dashed line in D shows the temporal development of the transverse steady state magnetization for the approximation of an infinitesimal short RF-pulse with identical parameters.

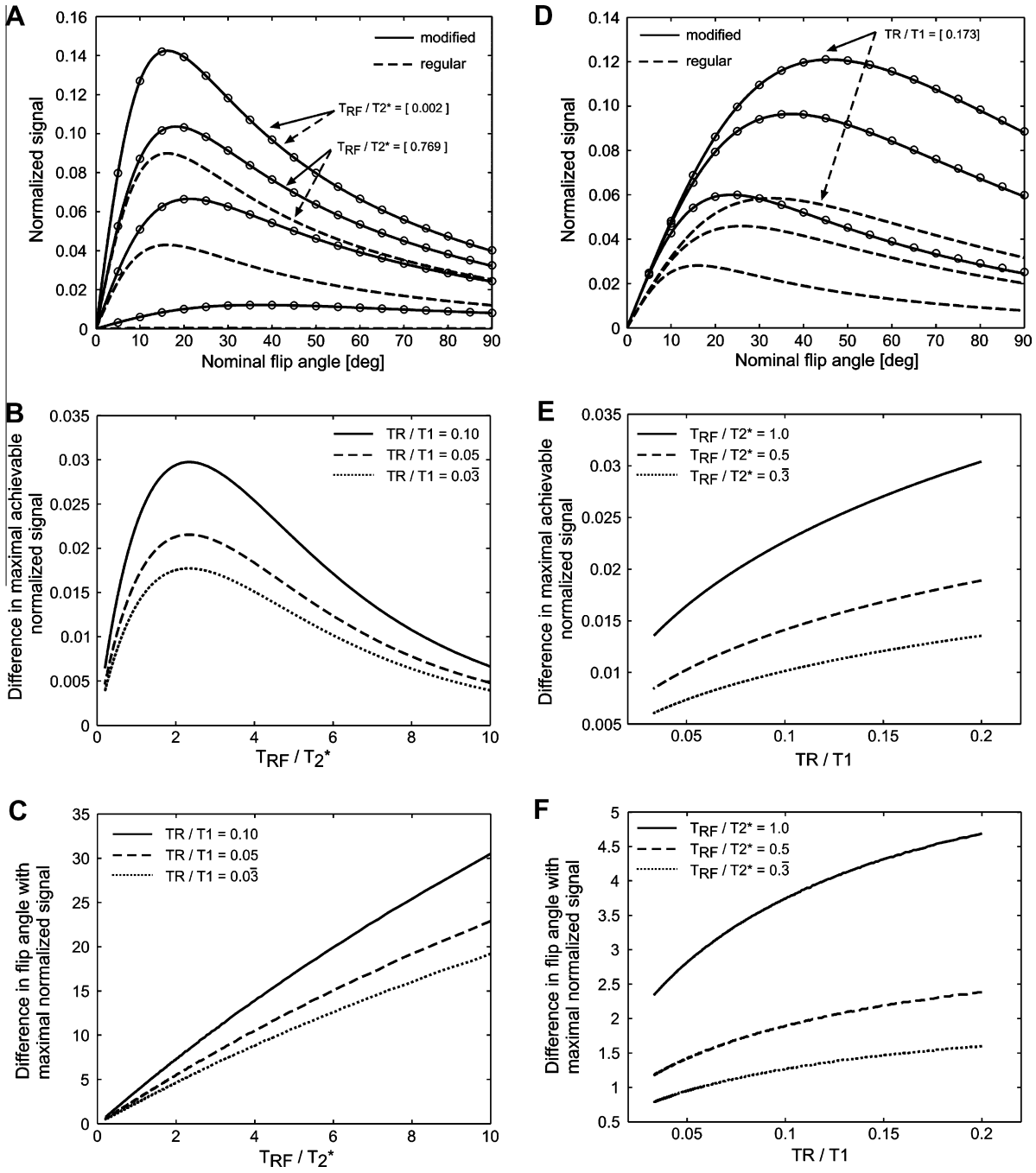

Fig. 3. Analytical solution of the steady state transverse magnetization, i.e. signal yield over a flip angle range from 0° to 90° showing the results of the regular Ernst equation as dotted lines, the results of the modified Ernst equation as solid lines. (A) Shows the results for variable $T2^*$ = (0.02, 0.1, 0.26, 100) ms at constant parameters T_{RF} = 0.2 ms, TE = 0.12 ms, TR = 6.1 ms, $T1$ = 150 ms. Results of $T_{RF}/T2^*$ = 0.002 and $T_{RF}/T2^*$ = 0.769 are indicated, the other two ratios ($T_{RF}/T2^*$ = 2 and $T_{RF}/T2^*$ = 10) are shown below. (D) Shows the result for variable TR = (6, 16, 26) ms at constant parameters $T2^*$ = 0.26 ms, T_{RF} = 0.8 ms, TE = 0.42 ms, $T1$ = 150 ms. Results of the investigated ratio TR/$T1$ = 0.173 are indicated, whereas results for the other two ratios (TR/$T1$ = 0.107 and TR/$T1$ = 0.04) are shown below. Circles in (A and D) represent the respective data obtained by numerical simulation. (B and E) Show the absolute difference in maximum achievable signal yield between the regular and modified Ernst equation. (C and F) Show the difference in the nominal flip angle leading to maximum signal yield (i.e. Ernst angle).

$T1 \gg T_{RF}$, all calculations with variable ratios of $T_{RF}/T2^*$ and TR/$T1$ led to similar results of the numerical simulation and the modified Ernst equation (Fig. 3A and D). Deviations between numerical simulation and modified Ernst equation became relevant (>∼2% at high nominal flip angles of 80–90°), if longitudinal relaxation time was only five times longer than the RF-pulse duration. This finding was independent of transverse in-pulse relaxation effects ($T2^*/T_{RF}$) or repetition time TR, exemplarily see Fig. 5. Thus, under conditions with relatively short $T1 \approx T_{RF}$, it is no longer possible to calculate exact $T1$ values based on the 'variable flip angle method' and the proposed modified Ernst equation.

4.3. Experimental results

Using an echo time increment of 0.1 ms, transverse relaxation time $T2^*$ could be estimated by assuming a mono-exponential signal decay for the investigated solid polymeric material (Fig. 6). This indicates that true transverse relaxation effects rather than

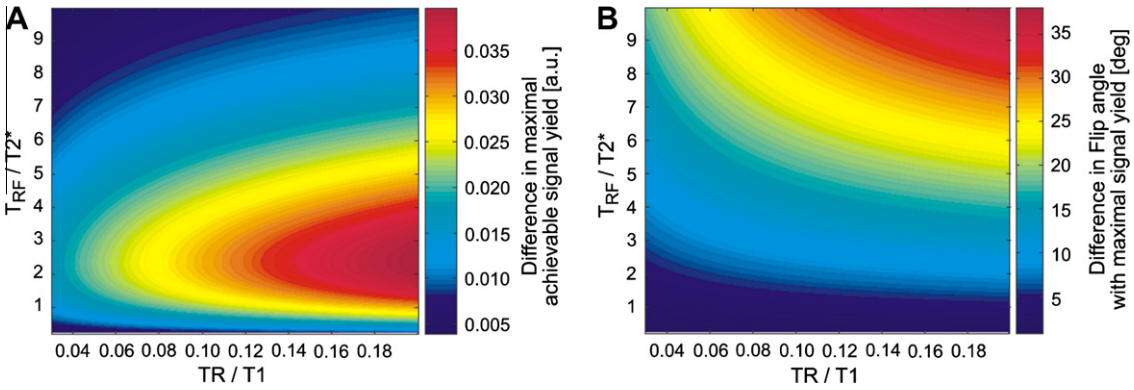

Fig. 4. (A) Shows the difference in maximum achievable signal yield between the regular and modified Ernst equation for a range of $T_{RF}/T2^*$ and TR/$T1$ combinations which can be observed in tissues and materials with extremely fast signal decay. (B) Shows the difference in the predicted flip angle with maximum signal yield (Ernst angle) between regular and modified Ernst equation.

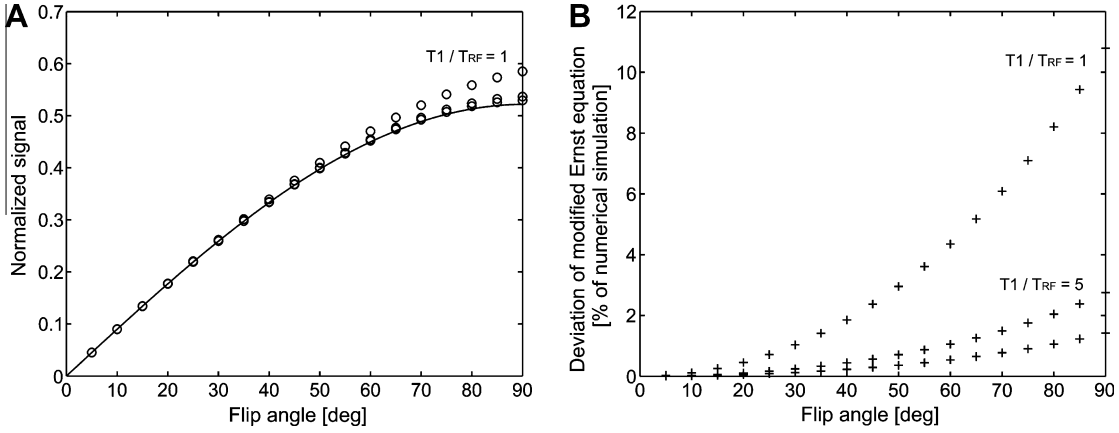

Fig. 5. (A) Circles represent normalized signal obtained from numerical simulation with different $T1/T_{RF}$ ratios ($T1/T_{RF}$ = 1, 5 10) at constant parameters T_{RF} = 0.1 ms, TR = 10 ms, $T2^*$ = 0.1 ms and TE = 0.07 ms. Results for $T1/T_{RF}$ = 1 are indicated, results of the other two ratios are shown below. Predicted signal from modified Ernst equation is shown as a solid line. (B) Shows the deviation between numerical and analytical signal yield for the investigated $T1/T_{RF}$ ratios. Results for $T1/T_{RF}$ = 1 or 5 are indicated, results of the ratio are shown below.

B_0-inhomogeneities are responsible for the signal decay. In Fig. 6, pixel-wise calculation of $T2^*$ shows a relatively homogenous distribution of values throughout the specimen with $T2^*$ = 295.6 ± 3.1 μs (arithmetic mean ± standard deviation). Maximum achievable nominal flip angles were 43°, 62° and again 62° at RF-pulse durations of T_{RF} = 0.1 ms, T_{RF} = 0.2 ms and T_{RF} = 0.4 ms, respectively. Maximum achievable nominal flip angles were limited due to restrictions in either the maximum allowed peak voltage of the RF excitation pulse (for T_{RF} = 0.1 ms) or SAR (for T_{RF} = 0.2 ms and T_{RF} = 0.4 ms).

Both, the modified as well as the regular Ernst equation (Eqs. (2) and (1), respectively) could be easily fitted to the signal intensity data for each measurement series at various flip angles (Fig. 7). Residual plots of both the regular and modified Ernst equation did not show marked differences in the fit quality for all three investigated RF-pulse durations. However, the resulting $T1$ relaxation times were quite different. Using previously determined $T2^*$ values, distribution maps of longitudinal relaxation times were calculated on a pixel-by-pixel basis. Relatively homogenous distribution of $T1$ values are depicted throughout the sample (Fig. 8). For the modified Ernst equation, calculated $T1$ values did not depend on the RF-pulse duration and can thus be regarded as accurate. In contrast, the use of the regular Ernst equation results in markedly shorter longitudinal relaxation times, if longer RF-pulse durations are used, which is unacceptable for a proper $T1$ measurement (Table 1).

5. Discussion

As shown in the presented work the approximation of a RF excitation pulse by a simple rotation matrix will become incorrect, if the effective transverse relaxation time $T2^*$ is in the range of the RF-pulse duration. Intuitively one might expect the following: For increasing values of τ and for the same nominal flip angle α, $T2^*$ relaxation during the RF-pulse reduces the obtained transverse magnetization, less longitudinal magnetization is rotated and a larger residual longitudinal magnetization remains.

However, if the echo time TE is also considered and TE is, as usually done, defined from the middle of an excitation pulse until acquisition of central k-space data, the resulting transverse magnetization is distinctly underestimated by the regular Ernst equation. This finding occurs due to the fact that transverse signal loss during a finite RF excitation pulse is always less pronounced than compared to the case of free relaxation after an infinitesimal short RF-pulse.

Consequently, if the echo time TE is fixed one should better use longer RF-pulses in order to increase signal yield. In contrast, shorter RF-pulses allow us to reduce the echo time TE, which is even more effective in terms of gaining higher signal amplitudes. If the RF-pulse duration is shortened too much, it may lead to another problem: the transmitter voltage, which is needed to achieve a specific nominal flip angle, might be beyond the capabilities of the MR system and thus imaging at the Ernst angle may not be

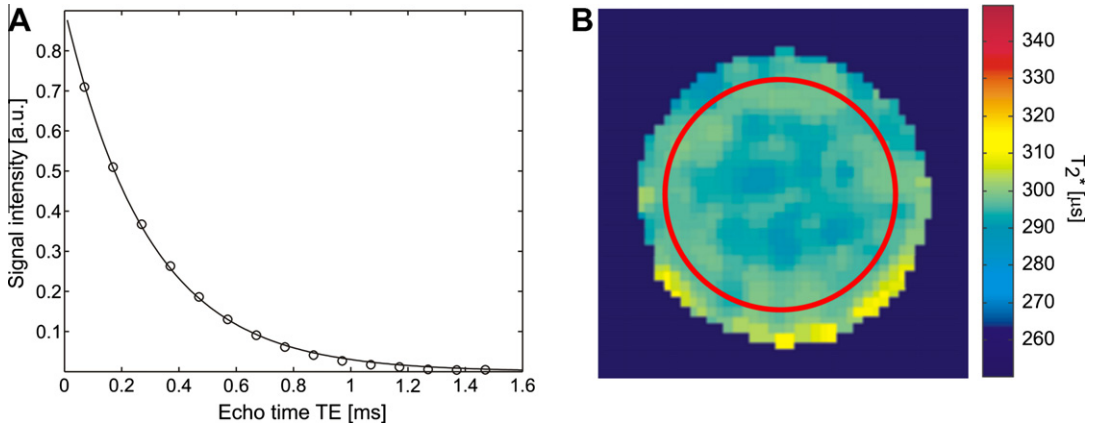

Fig. 6. A nearly mono-exponential signal decay of the investigated solid polymeric material polyurethane is shown in (A) (circles: measured mean signal yield at various echo times, solid line: two parameter fitted mono-exponential signal decay curve). A homogenous distribution of transverse relaxation time ($T2^*$) is revealed by the pixel-wise calculated $T2^*$-map in Figure 6B. The red circle within the polymeric sample indicates the region-of-interest which was used to estimate mean $T2^*$ ± standard deviation as shown in Table 1.

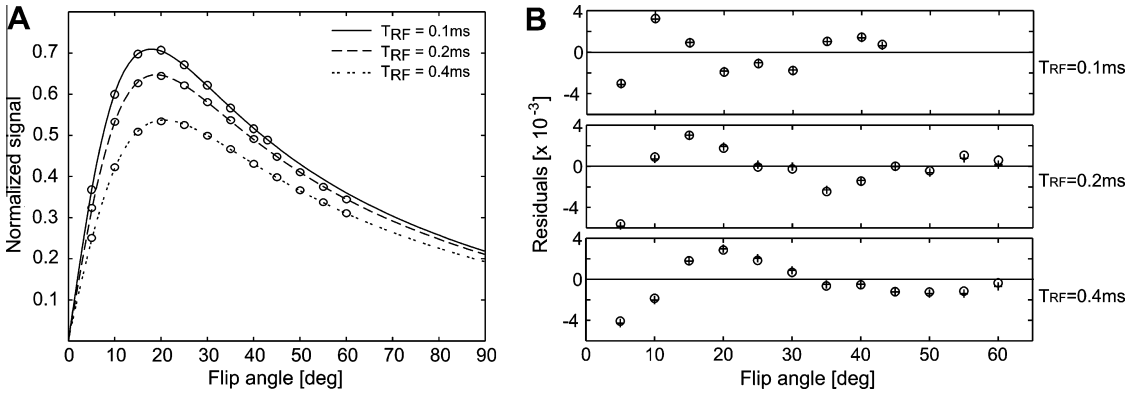

Fig. 7. (A) Shows observed signal intensity at various flip angles for three different RF-pulse durations. Solid lines represent fitted signal decay curves for both regular and modified Ernst equation. (B) Shows residuals for the fitting procedures of the three investigated pulse durations. Residuals of the regular Ernst equation are presented as circles, the ones of the modified Ernst equation as crosses.

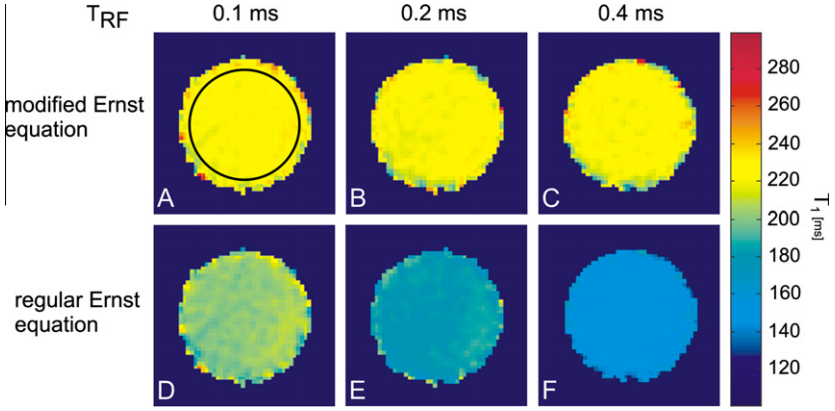

Fig. 8. Relatively homogenous distribution of longitudinal relaxation time ($T1$) of polyurethane in T_1-maps calculated on a pixel-by-pixel basis from images recorded with rectangular RF excitation pulse of duration T_{RF} = 0.1 ms (A, D), T_{RF} = 0.2 ms (B, E) and T_{RF} = 0.4 ms (C, F). Calculations were performed by means of the modified Ernst equation (A–C) and by means of the regular Ernst equation (D–F). The black circle in A indicates exemplarily the region-of-interest used for evaluation of arithmetic mean $T1$ ± standard deviation as presented in Table 1.

achieved. In this case, it might be better to broaden the RF-pulse slightly to increase signal intensity. Furthermore, one should also take into account that the nominal flip angle with the highest achievable transverse magnetization shifts to higher flip angles than predicted by the regular Ernst equation, if $T2^*$ approximates T_{RF}.

It must also be noted that the analytically derived modified Ernst equation for 3D UTE sequences describes signal yield only in a correct manner, if $T1$ is much longer than the duration of the RF excitation pulse T_{RF}. However, numerical simulations showed that the deviation between the analytically calculated signal yield and the numerical simulations is only ~2% at high flip angles, if $T1$ is five

Table 1
Experimental results for longitudinal relaxation times ($T1$) of solid polymeric material polyurethane (PUR).

	$T1$ (ms)		
	T_{RF} = 0.1 ms	T_{RF} = 0.2 ms	T_{RF} = 0.4 ms
Modified signal equation	224.8 ± 3.4	223.2 ± 3.7	224.8 ± 4.0
Regular signal equation	202.2 ± 3.3	181.8 ± 3.0	152.3 ± 2.6

T_{RF}: duration of rectangular RF excitation pulse; $T1$: longitudinal relaxation time.

times longer than T_{RF}. This finding was independent of a possible in-pulse relaxation of transverse magnetization. Since cortical bone and most solid polymeric materials show $T1$ values in the order of hundreds of milliseconds [2,13,15], longitudinal relaxation during RF excitation can be neglected at pulse durations of 0.1–0.4 ms. Furthermore, it has to be stated clearly that the presented modified Ernst equation is only valid for non-slice-selective, rectangular RF excitation pulses, which are usually applied in 3D UTE sequences.

In addition to relaxation of transverse magnetization during RF excitation, the relaxation during signal sampling is another factor, which hampers diagnostic image quality. It broadens the point spread function and thus limits the achievable resolution by pronounced blurring effects [8]. In 2D UTE sequences, working with shaped RF-pulses, transverse relaxation during RF excitation does not only influence signal yield and spatial resolution, but also reduces the quality of the slice profile [16–20]. Additionally applied RF-pulses for saturation of fatty tissue and long-$T2$ components might also hamper the in vivo applicability of the proposed modified Ernst equation [21–23]. The impact of those long-$T2$ preparation pulses on the signal yield from short-$T2$ components should be additionally investigated in future studies.

In the general case of off-resonant RF-pulses it is necessary to apply the equations reported by Mulkern and Williams [24]. Unfortunately, this more general approach leads to relatively complicated expressions, while the use of the clearly simpler modified Ernst equation – proposed in our work – seems sufficient in many practical cases.

For accurate assessment of longitudinal relaxation time $T1$, one has to previously determine the transverse relaxation time of the tissue or material investigated. Thus, $T1$ measurement has to be necessarily accompanied by an additional measurement of $T2^*$ or at least an estimation of transverse relaxivity. However, if tissues or materials with extremely fast signal decay are to be characterized by their relaxation times, one might measure the transverse relaxivity anyway.

On clinically used, whole-body MRI units transverse relaxation time $T2$ cannot be assessed using conventional spin-echo techniques in tissues or materials with extremely fast signal decay. Thus, the effective transverse relaxation time $T2^*$ was estimated by means of a 3D UTE sequence with variable delay time d_1. Generally, $T2^*$ is shorter or equal compared to the true spin–spin relaxation time $T2$. Since the investigated material PUR does not generate extensive field distortions based on susceptibility or dipolar effects, measured $T2^*$ values are expected to be mainly dominated by the spin–spin relaxation $T2$.

In many cases, especially regarding medical examinations of tendons, ligaments or cortical bone, but also in solid polymers, several different $T2$ (and $T2^*$) moieties may occur [25,26]. In those cases, mono-exponential signal fitting is critical and might lead to inappropriate $T2^*$ values and, as a consequence, also to hampered $T1$ measurements. However, for simplicity reasons a mono-exponential signal decay of the investigated solid polymeric sample was assumed.

In the experiments regarding the longitudinal relaxivity of the investigated sample, it was shown that both the regular and modified Ernst equation can be used for fitting signal intensities at various flip angles with almost identical residuals (Fig. 7). Thus, one can not easily determine – by estimating the quality of the fit – which equation is suitable. Using the regular Ernst equation, resulting longitudinal relaxation times were shown to be clearly dependent on RF-pulse duration. This finding reveals that reliable $T1$ measurements in specimen with considerable in-pulse relaxation are impossible, if in-pulse relaxation effects are not taken into account. In contrast, using the modified Ernst equation, effects of in-pulse relaxation are adequately compensated and calculation of longitudinal relaxation time from acquired data did not vary with RF-pulse durations ($T1$ = 224.8 ± 3.4 ms at T_{RF} = 0.1 ms and at T_{RF} = 0.4 ms: $T1$ = 224.8 ± 4.0 ms) as shown in Fig. 8 and Table 1.

In conclusion, the modified Ernst equation correctly accounts for transverse in-pulse relaxation effects and allows calculation of transverse magnetization in the steady state, if transverse relaxation time $T2^*$ of the investigated tissue is known. The modified Ernst equation is only valid for conditions with $T1$ clearly longer than T_{RF}, but this prerequisite is usually fulfilled for UTE examinations of materials or tissues with extremely short transverse relaxation times. Numerical simulations of the signal behavior and experiments with a solid polymeric material confirmed the analytically obtained results. Thus, the modified Ernst equation allows, by means of the 'variable flip angle' approach, calculation of longitudinal relaxation times in materials and tissues with extremely fast transverse relaxation.

Appendix 1

In order to derive a signal equation for spoiled GRE-sequences considering transverse relaxation with very short $T2^*$, the Bloch equations have to be solved during an on-resonant rectangular pulse. The direction of the pulse only influences the phase of the steady state transverse magnetization and not the magnitude. Therefore, w.l.o.g. a pulse is assumed in x-direction with amplitude B and duration T_{RF} considering transverse relaxation during application of the pulse described by $T2^*$. The Bloch equations denote

$$\frac{d\vec{M}}{dt} = (\widehat{\omega_x} - \widehat{R})\vec{M} + R1 \cdot M_\infty \vec{e}_z$$

with

$$\widehat{\omega_x} = \begin{pmatrix} 0 & 0 & 0 \\ 0 & 0 & \gamma B \\ 0 & -\gamma B & 0 \end{pmatrix}$$

and

$$\widehat{R} = \begin{pmatrix} R2^* & 0 & 0 \\ 0 & R2^* & 0 \\ 0 & 0 & R1 \end{pmatrix}$$

where $R1$: = $1/T1$, $R2^*$: = $1/T2^*$ and M_∞ is the longitudinal equilibrium magnetization in z-direction.

Although the following computations could also be carried out for arbitrary $R1$ and $R2^*$ (see comment below), longitudinal relaxation will be ignored, i.e. $R1 = 0$ is assumed in order to simplify the calculation and expressions. This is justified by the fact that in many practical applications $T1$ is much longer than T_{RF}.

By setting $\widehat{A} := \widehat{\omega_x} T_{RF} - \widehat{R} T_{RF}$, the (formal) solution of the Bloch equations above at time T_{RF} is given by $\vec{M}(T_{RF}) = \exp(\widehat{A})\vec{M}_0$ where $\vec{M}_0$ is the initial magnetization at time $t = 0$. To get an explicit solution $\exp(\widehat{A})$ has to be calculated. By defining the two-dimensional matrix

$$\widehat{\Sigma} = \begin{pmatrix} -\frac{R2^*}{2} T_{RF} & \alpha \\ -\alpha & \frac{R2^*}{2} T_{RF} \end{pmatrix},$$

where $\alpha := \gamma B T_{RF}$ is the flip angle, $\widehat{A}$ and $\exp(\widehat{A})$ can be expressed as

$$\widehat{A} = \begin{pmatrix} -R2^* T_{RF} & 0\ 0 \\ 0 & -\frac{R2^*}{2} T_{RF}\,\widehat{I} + \widehat{\Sigma} \\ 0 & \end{pmatrix}$$

and

$$\exp(\widehat{A}) = \begin{pmatrix} \exp(-R2^* T_{RF}) & 0\ 0 \\ 0 & \exp\left(-\frac{R2^*}{2} T_{RF}\right) \exp\left(\widehat{\Sigma}\right) \\ 0 & \end{pmatrix},$$

where $\widehat{I}$ is the two-dimensional unity matrix.

With $\Sigma^2 = -\Phi^2 \widehat{I}$, where $\Phi := \sqrt{\alpha^2 - \tau^2}$ and $\tau := \frac{R2^*}{2} T_{RF}$, it follows $\widehat{\Sigma^{2n}} = (-1)^n \Phi^{2n} \widehat{I}$ and $\widehat{\Sigma^{2n+1}} = (-1)^n \Phi^{2n} \widehat{\Sigma}$. With aid of the series expansion of the exponential, sine and cosine functions, $\exp(\widehat{\Sigma})$ can be explicitly calculated obtaining

$$\exp(\widehat{\Sigma}) = \begin{pmatrix} \cos(\Phi) - \frac{\tau}{\Phi} \cdot \sin(\Phi) & \frac{\alpha}{\Phi} \cdot \sin(\Phi) \\ -\frac{\alpha}{\Phi} \cdot \sin(\Phi) & \cos(\Phi) + \frac{\tau}{\Phi} \cdot \sin(\Phi) \end{pmatrix}.$$

By using $\exp(\widehat{A})$ instead of the rotation matrix $\widehat{R_x}(\alpha)$ for the calculation of the steady state signal, setting $E1 = \exp(-TR/T1) \approx \exp(-(TR - T_{RF})/T1)$ for the free relaxation term and defining TE as time from the centre of the RF-pulse until acquisition of central k-space data the following equation results.

$$M_{ss} = M_\infty \frac{(1 - E1)}{1 - E1 \cdot \exp(-\tau) \cdot [\cos(\Phi) + \frac{\tau}{\Phi} \cdot \sin(\Phi)]} \cdot \exp(-\tau) \cdot \frac{\alpha}{\Phi} \cdot \sin(\Phi) \cdot \exp(-(TE/T2^* - \tau)),$$

which is the same expression as in Eq. (2).

Without ignoring longitudinal relaxation described by $R1$ the Bloch equations become a system of inhomogeneous differential equations, which could principally be analytically solved the same way as described above by explicit calculation of $\exp(\widehat{A})$ in the formal solution of the inhomogeneous differential equation and by using the identity

$$\begin{pmatrix} -R2^* T_{RF} & \alpha \\ -\alpha & -R1 T_{RF} \end{pmatrix} = -\frac{R2^* + R1}{2} T_{RF}\,\widehat{I} + \begin{pmatrix} -\frac{R2^* - R1}{2} T_{RF} & \alpha \\ -\alpha & \frac{R2^* - R1}{2} T_{RF} \end{pmatrix},$$

leading, however, to more elongate expressions. For a general analytical solution of the Bloch equations including relaxation and off-resonant RF-pulses see Ref. [24].

References

[1] M.D. Robson, G.M. Bydder, Clinical ultrashort echo time imaging of bone and other connective tissues, NMR Biomed. 19 (2006) 765–780.

[2] F. Springer, P. Martirosian, N.F. Schwenzer, M. Szimtenings, P. Kreisler, C.D. Claussen, F. Schick, Three dimensional ultrashort echo time imaging of solid polymers on a 3 T whole-body MRI-scanner, Invest. Radiol. 43 (2008) 802–808.

[3] D.J. Tyler, M.D. Robson, R.M. Henkelman, I.R. Young, G.M. Bydder, Magnetic resonance imaging with ultrashort TE (UTE) PULSE sequences: technical considerations, J. Magn. Reson. Imag. 25 (2007) 279–289.

[4] P.D. Gatehouse, R.W. Thomas, M.D. Robson, G. Hamilton, A.H. Herlihy, G.M. Bydder, Magnetic resonance imaging of the knee with ultrashort TE pulse sequences, Magn. Reson. Imag. 22 (2004) 1061–1067.

[5] F. Springer, P. Martirosian, J. Machann, N.F. Schwenzer, C.D. Claussen, F. Schick, Magnetization transfer contrast imaging in bovine human cortical bone applying an ultrashort echo time sequence at 3 T, Magn. Reson. Med. 61 (2009) 1040–1048.

[6] S. Nielles-Vallespin, M.A. Weber, M. Bock, A. Bongers, P. Speier, S.E. Combs, J. Wohrle, F. Lehmann-Horn, M. Essig, L.R. Schad, 3D radial projection technique with ultrashort echo times for sodium MRI: clinical applications in human brain and skeletal muscle, Magn. Reson. Med. 57 (2007) 74–81.

[7] P.T. Gurney, B.A. Hargreaves, D.G. Nishimura, Design and analysis of a practical 3D cones trajectory, Magn. Reson. Med. 55 (2006) 575–582.

[8] J. Rahmer, P. Bornert, J. Groen, C. Bos, Three-dimensional radial ultrashort echo-time imaging with *T2* adapted sampling, Magn. Reson. Med. 55 (2006) 1075–1082.

[9] J. Du, M. Bydder, A.M. Takahashi, C.B. Chung, Two-dimensional ultrashort echo time imaging using a spiral trajectory, Magn. Reson. Imag. 26 (2008) 304–312. Epub 2007 Dec 2021.

[10] J. Frahm, A. Haase, D. Matthaei, Rapid three-dimensional MR imaging using the FLASH technique, J. Comput. Assist. Tomogr. 10 (1986) 363–368.

[11] A. Haase, J. Frahm, D. Matthaei, W. Hänicke, K.D. Merboldt, FLASH imaging: rapid imaging using low flip angle pulses, J. Magn. Reson. 67 (1986) 256.

[12] E.K. Fram, R.J. Herfkens, G.A. Johnson, G.H. Glover, J.P. Karis, A. Shimakawa, T.G. Perkins, N.J. Pelc, Rapid calculation of *T1* using variable flip angle gradient refocused imaging, Magn. Reson. Imag. 5 (1987) 201–208.

[13] S. Widmaier, W.I. Jung, K. Pfeffer, M. Pfeffer, O. Lutz, MRI and determination of *T1* and *T2* of solid polymers using a 1.5 T whole-body imager, Magn. Reson. Imag. 11 (1993) 733–737.

[14] A.J. Miller, P.M. Joseph, The use of power images to perform quantitative analysis on low SNR MR Images, Magn. Reson. Imag. 11 (1993) 1051–1056.

[15] D.E. Axelson, A. Kantzas, A. Nauerth, H magnetic resonance imaging of rigid polymeric solids, Solid State Nucl. Magn. Reson. 6 (1996) 309–321.

[16] F. Staehle, S. Nielles-Vallespin, A. Bongers, L.R. Schad, Slice profile measurements of half pulse excitation for MR-imaging with ultra-short echo times (UTE), Z. Med. Phys. 16 (2006) 200–207.

[17] J.M. Pauly, B.L. Daniel, K.M. Pauly, Double half RF pulses for reduced sensitivity to eddy currents in UTE imaging, Magn. Reson. Med. 61 (2009) 1083–1089.

[18] S. Josan, E. Kaye, J.M. Pauly, B.L. Daniel, K.B. Pauly, Improved half RF slice selectivity in the presence of eddy currents with out-of-slice saturation, Magn. Reson. Med. 61 (2009) 1090–1095.

[19] S. Josan, J.M. Pauly, B.L. Daniel, K.B. Pauly, Double half RF pulses for reduced sensitivity to eddy currents in UTE imaging, Magn. Reson. Med. 61 (2009) 1083–1089.

[20] A. Lu, B.L. Daniel, J.M. Pauly, K.B. Pauly, Improved slice selection for *R2*∗ mapping during cryoablation with eddy current compensation, J. Magn. Reson. Imag. 28 (2008) 190–198.

[21] P.E. Larson, P.T. Gurney, K. Nayak, G.E. Gold, J.M. Pauly, D.G. Nishimura, Designing long-*T2* suppression pulses for ultrashort echo time imaging, Magn. Reson. Med. 56 (2006) 94–103.

[22] P.E.Z. Larson, S.M. Conolly, J.M. Pauly, D.G. Nishimura, Using adiabatic inversion pulses for long-*T2* suppression in ultrashort echo time (UTE) imaging, Magn. Reson. Med. 58 (2007) 952–961.

[23] J. Rahmer, U. Blume, P. Börnert, Selective 3D ultrashort TE imaging: comparison of "dual-echo" acquisition and magnetization preparation for improving short-*T2* contrast, Magma 20 (2007) 83–92.

[24] R.V. Mulkern, M.L. Williams, The general solution to the Bloch equation with constant RF and relaxation terms: application to saturation and slice selection, Med. Phys. 20 (1993) 5–13.

[25] W. Kuhn, P. Barth, S. Hafner, G. Simon, H. Schneider, Material properties imaging of cross-linked polymers by NMR, Macromolecules 27 (1994) 5773–5779.

[26] P.W. Anderson, P.R. Weiss, Exchange narrowing in paramagnetic resonance, Rev. Mod. Phys. 25 (1953) 269–276.